Impaired integrity of the brain parenchyma in non-geriatric patients with major depressive disorder revealed by diffusion tensor imaging

Abstract

Diffusion tensor imaging (DTI) is considered to be able to non-invasively quantify white matter integrity. This study aimed to use DTI to evaluate white matter integrity in non-geriatric patients with major depressive disorder (MDD) who were free of antidepressant medication. DTI was performed on 19 non-geriatric patients with MDD, free of antidepressant medication, and 19 age-matched healthy subjects. Voxel-based and histogram analyses were used to compare fractional anisotropy (FA) and mean diffusivity (MD) values between the two groups, using two-sample *t* tests. The abnormal DTI indices, if any, were tested for correlation with disease duration and severity, using Pearson product-moment correlation analysis. Voxel-based analysis showed clusters with FA decrease at the bilateral frontal white matter, anterior limbs of internal capsule, cerebellum, left putamen and right thalamus of the patients (uncorrected $P < 0.001$). Histogram analysis revealed lower peak position of FA histograms in the patients ($P = 0.00097$). FA values of the abnormal clusters and peak positions of FA histograms of the patients exhibited moderate correlation with disease duration and severity ($P < 0.05$). These results suggest implication of frontal-subcortical circuits and cerebellum in MDD, and the potential utility of FA in evaluation of brain parenchymal integrity.

Keywords

Fractional anisotropy

Mean diffusivity

Voxel-based analysis

Histogram

1. Introduction

Major depressive disorder (MDD) is a common disorder with a chronic pattern of recurrence and a lifetime prevalence of 16.2% (Kessler et al., 2003). It is the fourth most disabling medical condition worldwide based on disability-adjusted life years (Greenberg et al., 1993). The neurobiology of MDD is not completely understood. A number of previous studies involving morphometric analysis using optical dissector methodology, voxel-based morphometry using magnetic resonance imaging (MRI), single photon emission computed tomography (SPECT), and positron emission tomography (PET) have reported a reduction in cortical thickness and the density of cortical neurons, as well as alterations in cerebral blood flow or glucose metabolism of cerebral cortices in MDD. These results are suggestive of gray matter pathology (Graff-Guerrero et al., 2004; Uranova et al., 2004; Egger et al., 2008; Fujimoto et al., 2008). On the other hand, recent converging evidence based on the findings of diffusion tensor imaging (DTI) is suggestive of abnormalities of white matter or frontal-subcortical circuits (e.g. Tekin and Cummings., 2002; Bae et al., 2006; Nobuhara et al., 2006; Shimony et al., 2009).

DTI is an MRI technique which can quantify white matter integrity noninvasively and in vivo (Moseley, 2002). This technique enables quantification of white matter integrity through its ability to detect motion of water molecules. Many studies suggest that DTI can uncover the microstructural white matter abnormalities that cannot be detected by other MRI techniques (e.g. Nagesh et al., 2008; Tha et al., 2010). It has also been reported that the abnormalities revealed by DTI correlate significantly with clinical severity in various white matter pathologies (e.g. Della Nave et al., 2007; Tha et al., 2010). Two major indices

– fractional anisotropy (FA) and mean diffusivity (MD), are usually used to quantify microstructural white matter integrity by DTI (Moseley, 2002). FA quantifies the degree of directional coherence, whereas MD quantifies the degree of magnitude of water diffusion. The major DTI indices are usually evaluated by either one or more of the following techniques: region-of-interest (ROI)-based analysis, tract (tractography)-based analysis, histogram analysis, and voxel-based analysis (Jones et al., 2005; Taoka et al., 2007). ROI-based and tract (tractography)-based analyses are usually chosen if there is known targeted anatomical area or tract to be evaluated. The latter two techniques are better suited if the area of involvement is not known, or when an *a priori* spatial selection and hypothesis are not made. In addition, the latter two techniques do not involve placement of ROI — which requires an operator with expertise in neuroanatomy and involves some inherent subjectivity (Marquez de la Plata et al., 2011). Previous DTI studies on MDD have been performed using ROI-based analysis, voxel-based analysis, and/ or tract (tractography)-based analysis (e.g. Taylor et al., 2004; Malykhin et al., 2008; Korgaonkar et al., 2011; Wu et al., 2011). Regarding selection of patients, the majority of these studies were performed on geriatric patients and the patients under antidepressant medication (e.g. Alexopoulos et al., 2002; Yang et al., 2007; Alexopoulos et al., 2008; Zou et al., 2008). The results of these studies revealed impaired white matter integrity in these patients. However, it is possible that the findings of these studies were confounded by age-related pathology and/ or the effect of antidepressant medication (Korgaonkar et al., 2011). With aging, the FA values of all white matter tracts decrease and their MD values increase (Sala et al., 2012). There have also been a few reports about the effect of antidepressant medication on white matter

integrity (Yoo et al., 2007; Sijens et al., 2008; Taylor et al., 2011). Normalization of FA and MD values of cerebral white matter after treatment with antidepressants such as citalopram, fluoxetine, and sertraline, as well as decrease in the FA values of the right posterior thalamic radiation following treatment with citalopram, have been documented — suggestive of the modification of white matter integrity by antidepressant medication. The number of DTI studies performed on non-geriatric patients who were free of antidepressant medication is limited (Li et al., 2007; Ma et al., 2007; Korgaonkar et al., 2011; Ouyang et al., 2011; Wu et al., 2011; Zhu et al., 2011). Although the results of these preliminary studies suggest impaired white matter integrity in MDD, the location of abnormalities is inconsistent among the studies and their results are not replicable (Korgaonkar et al., 2011; Wu et al., 2011) — calling for the need for further investigations.

This study was aimed to evaluate white matter integrity in non-geriatric (e.g., <65 years) patients with MDD who were free of antidepressant medication for at least 6 months, by using voxel-based and histogram analyses of DTI. It was hypothesized that these patients would have impaired integrity of white matter that could be depicted by DTI.

2. Methods

2.1. Participants

This prospective study was approved by the local institutional review board. Written informed consent was obtained from all participants.

The patients were recruited during a 35-month period (August, 2007 to March' 2010), at the Department of Psychiatry, Hokkaido University Hospital. Inclusion criteria for

the patients were age between 20 and 64 years (Waxman et al., 1982; Korgaonkar et al., 2011), diagnosis of MDD according to the Diagnostic and Statistical Manual, Fourth Edition, Text Revision (DSM-IV-TR), and being free of antidepressant medication for at least 6 months. Exclusion criteria were absolute contraindications for MRI, comorbid axis I or II disorders, history of electroconvulsive therapy, history of diseases that might affect white matter integrity (e.g. infarct, hemorrhage, migraine), and significant abnormality on conventional MRI sequences {i.e., T2-weighted imaging (T2WI) and fluid-attenuated inversion recovery (FLAIR) imaging sequences}. Of 25 patients who fit the inclusion criteria, 19 patients were eligible for the study. No patients had any psychotic features. Eleven patients were never treated with antidepressants. The remaining eight patients had a previous history of medication with one or more antidepressant agents, but had been free of the medication for at least 6 months.

To obtain normal control data, MRI was also performed on 19 age-matched normal subjects. Exclusion criteria were absolute contraindications for MRI, axis I or II disorders, history of diseases that might affect white matter integrity, and any obvious abnormality on the conventional MRI sequences. Psychiatric diseases were excluded through a short-structured diagnostic interview (Mini-International Neuropsychiatric Interview; MINI)(Sheehan et al., 1998).

The demographic characteristics of the patients and control subjects are summarized in Table 1.

2.2. MRI

In all patients, MRI was performed on the day of first clinical consultation for the current episode or the day on which the diagnosis was made. There was no undue delay in the prescription of antidepressant medication for the purpose of this study.

MRI was performed using a 1.5-T imager and a standard head coil. The participants were asked not to move their heads during the examination, and foam pads were used to minimize involuntary head motion. An axial single-shot spin-echo echo-planar imaging sequence was used for DTI. Parameters included the following: repetition time (TR)/echo time (TE), 5100/139 ms; b value (b), 1000 s mm^{-2}; diffusion-encoding gradients, 12 directions; number of signals acquired, two; field of view (FOV), 240 x 240 mm; matrix size, 128 x 128 (interpolated into 256 x 256); pixel size, 1.875 x 1.875 mm; intersection gap, 1.5 mm; section thickness, 5 mm; and section number, 23. Echo-planar images with no diffusion weighting (b = 0 s mm^{-2}) were also obtained for use in spatial normalization and coregistration.

In addition to DTI, axial fast spin-echo T2WI (TR/TE, 4540/96 ms; effective echo train length (ETL_{eff}), 7; FOV, 180 x 240 mm; matrix size, 185 x 448; pixel size, 0.973 x 0.536; intersection gap, 1.5 mm; section thickness, 5 mm; and section number, 23), axial fast FLAIR imaging (TR/TE, 9000/104 ms; inversion time (TI), 2500 ms; FOV, 180 x 240 mm; matrix size, 192 x 256; pixel size, 0.938 x 0.938; intersection gap, 1.5 mm; section thickness, 5 mm; and section number, 23), and three-dimensional T1-weighted imaging with a magnetization-prepared rapid acquisition gradient-echo (MPRAGE) sequence (TR/TE, 1900/3.9 ms; TI, 1100 ms; flip angle, 15°; FOV, 250 x 250 mm; matrix size, 256 x

256; pixel size, 0.978 x 0.978; gapless; section thickness, 1 mm; imaging plane, coronal; and section number, 240) were also acquired.

2.3. Image processing and analysis

2.3.1. Construction of FA and MD maps

FA and MD maps were constructed on a workstation from the diffusion tensor images, according to the methods of Basser and Pierpaoli (1996) (Dr.View/LINUX R2.5.0; AJS, Tokyo, Japan). To ensure computation only of tensors inside the brain rather than the surrounding air, a brain mask, computed based on the signal intensity of diffusion tensor images, was applied to the diffusion tensor images.

2.3.2. Voxel-based analysis

The steps involved all closely followed those of a previous report (Tha et al., 2010). First, the customized FA and MD templates were built from the FA and MD maps of the control subjects. For this purpose, the echo-planar images with no diffusion weighting of each control subject were first warped to the standard echo-planar template of statistical parametric mapping software (SPM5, www.fil.ion.ucl.ac.uk), by using default parameters. This transformation information was then applied to the FA and MD maps of each subject. The warped FA and MD maps were averaged and smoothed with a 6-mm full-width half-maximum (FWHM) Gaussian kernel, to form the customized FA and MD templates. Visual review of the output images was performed to ensure that no obvious registration error was encountered.

Next, the native FA and MD maps of all patients and control subjects were warped to the customized FA and MD templates, respectively. The parameters applied were the same as those described previously. Visual review of all warped images was performed to ensure that no obvious registration error was encountered. Individual maps were then smoothed with a 6-mm FWHM Gaussian kernel.

Warped and smoothed FA and MD maps of the patients and control subjects were next compared voxel-by-voxel by using a two-sample *t* test. The analysis was restricted to the area covered by a mask (void of cortical gray matter and ventricles) — which was developed from the customized FA template by discarding voxels with an FA value of less than 0.2 (MRIcron, www.cabiatl.com/mricro/mricron). Uncorrected *P* value of less than *0.001* and a cluster size of greater than 50 voxels were considered significant. The FA and MD values of the clusters in the patients which differed significantly from the control subjects, if any, were measured (MarsBaR, www.marsbar.sourceforge.net).

2.3.3. Histogram analysis

The steps involved were the same as those of a previous report (Mori et al., 2008), except that white matter masks were used in this study instead of whole-brain binary masks. In brief, the axial sections of individual MPRAGE images of each participant were coregistered to the echo-planar images with no diffusion weighting (SPM5). Visual review of the output images was performed to ensure that no obvious registration error was encountered. From the axial sections of the MPRAGE images, white matter was automatically segmented by using the default parameters of SPM5. Each segmented image

was checked to ensure accuracy. The segmented white matter (the segmented area also included the thalami and part of basal ganglia.) was used to serve as individual white matter masks. Each white matter mask was applied to the FA and MD maps of the corresponding participant (MRIcron). Histograms were then calculated for the masked FA and MD maps of each participant (ImageJ, www.rsb.info.nih.gov/ij). The bin width of the FA histograms was set as 0.01(between 0.0 and 1.0), and that of MD histograms was set as 5×10^{-5} (between 0.0 and 0.0055). To correct skewness, the natural logarithmic transformation of FA and MD bins was used. To correct for individual differences in the brain volume, each histogram was normalized by the total number of voxels contributing to the histogram. From each histogram, the peak height and location were extracted. These histogram parameters were then compared between the two groups, by using two-sample *t* test. A *P* value of less than *0.05* was set to determine statistical significance.

2.3.4. Correlation between the altered DTI indices and clinical variables

The absolute values of altered DTI indices of the patients (for voxel-based analysis, FA or MD values of the clusters which differed significantly from the control subjects; for histogram analysis, the peak height or position of FA or MD histograms which differed significantly from the control subjects), if any, were tested for correlation with total disease duration, duration of current disease episode, the scores that assess clinical severity {17-item Hamilton depression rating scale (HDRS-17) (Williams., 1988), global assessment of functioning (GAF)(Hall., 1995), Montgomery-Ásberg depression rating scale (MADRS) (Montgomery and Åsberg., 1979), clinical global impression-severity (CGIS)(Guy., 1976)},

and age, by using Pearson product-moment correlation analysis. The difference in the absolute values of altered DTI indices between the gender groups was evaluated by using two-sample *t* test. For all conditions, a *P* value of less than *0.05* was considered to indicate a significant difference. Correction for multiple comparisons was not performed.

3. Results

3.1. Voxel-based analysis

The results of voxel-by-voxel comparison of FA values between the two groups are shown in Fig. 1. Clusters with a significant decrease in FA values were observed at the bilateral frontal white matter, anterior limbs of the internal capsule, the left putamen, the mediodorsal nucleus of the right thalamus, and the anterior and superior aspect of bilateral cerebellar hemispheres of the patients. These clusters persisted even after controlling for age and gender. There were no significant clusters with an increase in the FA or altered MD values in the patients.

3.2. Histogram analysis

The mean FA and MD histograms of the patients and control subjects are shown in Fig. 2 and Fig. 3, respectively. The peak position of the FA histograms of the patients was significantly lower than that of the control subjects ($P=0.00097$). The results revealed a tendency toward a higher peak height in the MD histograms of the patients, but this alteration was not statistically significant ($P=0.11615$). The peak height of the FA

histograms and the peak position of the MD histograms did not vary significantly between the two groups (*P=0.79527* and *P =1*, respectively).

3.3. Correlation between the altered DTI indices and clinical variables

The results of the tests of correlation between the altered DTI indices of the patients and clinical variables are summarized in Table 2 and Fig. 4. Of clusters with a significant FA decrease, the FA value of the right frontal white matter (x = 12, y = 43, z = -18) revealed moderate negative correlation with duration of current disease episode. The right frontal white matter (x = 37, y = -19, z = 59) and the right anterior limb of internal capsule revealed moderate negative correlation with the GAF. The left anterior limb of the internal capsule exhibited a moderate positive correlation with total disease duration. The right cerebellar hemisphere exhibited a moderate positive correlation with the HDRS-17. The peak position of the FA histogram had a moderate positive correlation with total disease duration and the duration of the current disease episode. The FA value of the left cerebellar hemisphere revealed a moderate positive correlation with age. There was no significant difference in the regional FA values or the peak positions of FA histograms, between the gender groups (*P > 0.220*).

4. Discussion

This study evaluated white matter integrity in non-geriatric patients with MDD by using DTI. Two semiautomated/ automated methods — voxel-based and histogram analyses, were used for the analysis. Both methods were able to identify abnormalities in

the patients. Voxel-based analysis showed clusters with a significant decrease in FA at the bilateral frontal white matter and the anterior limbs of internal capsule. In addition to cerebral white matter, clusters with a significant decrease in the FA were also observed in the subcortical gray matter (including the left putamen and the mediodorsal nucleus of the right thalamus) and bilateral cerebellar hemispheres. In histogram analysis, a lower peak position (i.e. "shift toward the left") of the FA histograms of the patients was observed, indicative of inclusion in the patients with a greater number of voxels with low FA values compared to normal subjects.

Decrease in the FA is reflective of an impaired directional coherence of the brain microstructures (Moseley, 2002). The histological correlates of decrease in the FA, as revealed by the reports of autopsies and biopsies of various diseases of the brain and experimental models, include larger axonal spacing, a decrease in axon count, diameter and density, and myelin loss (Beaulieu, 2011). The autopsy reports of patients with MDD are scarce. Limited evidence has suggested myelin pallor in the white matter underlying prefrontal cortex (Regenold et al., 2007). Taken together with the knowledge that myelin pallor results from demyelination, incomplete myelination of axons, axonal loss, or axonal agenesis, our finding of FA decrease in the bilateral frontal white matter and anterior limbs of internal capsule may reflect axon and/ or myelin abnormality. Histological proof regarding the changes of the putamen, thalamus, and cerebellar hemispheres in MDD is lacking. The exact pathological process that occurs in these structures is thus not known. Nonetheless, from the findings of neuronal loss in some subcortical structures such as the nucleus basalis, substantia nigra, and raphe nucleus (Tsopelas et al., 2011), it is possible

that similar pathological changes are encountered. Axon and/ or myelin abnormality are also possible, as axon and myelin are the components of these structures.

Human behaviors (executive functions, social behavior, and motivational states) are mediated mainly by three parallel frontal-subcortical circuits (Tekin and Cummings, 2002). These circuits originate from the dorsolateral prefrontal region, lateral orbitofrontal region, and anterior cingulate portion of the frontal cortex; and form connections to the striatum, basal ganglia, and thalamus. From the thalamus, fibers of these circuits loop back to the cortex of origin. In addition to forming closed loops, these circuits form open connections with the other areas of the frontal lobe, parietal and temporal lobes, amygdala, hippocampus, substantia nigra, subthalamic nucleus, hypothalamus, and the brainstem. Our findings of decrease in the FA at the bilateral frontal white matter, anterior limbs of internal capsule, left putamen and right thalamus are suggestive of impaired integrity or dysfunctioning of these circuits. Although mediation of human behavior by these circuits is well-established, emerging evidence is suggestive of participation of the cerebellum in the regulation of mood and cognition as well (Diamond, 2000). The cerebellum forms anatomical and functional connections with the prefrontal cortex, subcortical limbic structures, and monoamine-producing brainstem nuclei (Konarski et al., 2005; Strick et al., 2009). Altered cerebellar levels of glial fibrillary acidic proteins (GFAP) have been observed in the patients with MDD (Fatemi et al., 2004). PET and functional MRI studies have also uncovered distinct variations in cerebellar activity between the patients with MDD and normal subjects (e.g. Dolan et al., 1992; Beauregard et al., 1998; Videbech et al.,

2001). Our finding of decrease in the FA in the bilateral cerebellar hemispheres is also supportive of implication of the cerebellum in the neuropathology of MDD.

Previous DTI studies on non-geriatric patients with MDD who were free of antidepressant medication have reported decreases in the FA in the white matter of the superior longitudinal fasiculus, cingulate, sagittal stratum, posterior thalamic radiation, anterior limb and retrolenticular part of the internal capsule, external capsule, splenium of the corpus callosum, stria terminalis, and the other subcortical and deep white matter of the frontal, parietal and temporal lobes (Li et al., 2007; Ma et al., 2007; Korgaonkar et al., 2011; Ouyang et al., 2011; Wu et al., 2011; Zhu et al., 2011). Added to these are our findings of the decrease in the FA in the left putamen, the mediodorsal nucleus of the right thalamus, and the bilateral cerebellar hemispheres. Taken together, these findings are suggestive of heterogeneity in the areas of the brain that are involved in MDD. It is possible that such heterogeneity arises from a variation in the circuits that are severed among the study population. From our finding of abnormalities in the frontal white matter and mediodorsal nucleus of the thalamus, it is thought that the dorsolateral prefrontal or orbitofrontal circuit is at least involved in our patients (Tekin and Cummings, 2002). Further stratification of analysis based on clinical symptoms may render more consistent results; however, variation in the exact anatomical location of the abnormalities along a single circuit (i.e. in terms of MNI or Tailairach coordinates) would remain unsolved (Blood et al., 2010).

In this study, histogram analysis of FA and MD was also performed, as a supplemental analysis to voxel-based analysis. To our knowledge, this is the first study that

has applied a histogram analysis of DTI in psychiatric diseases. This technique involves the creation of a frequency distribution showing the proportion of voxels in an image within a given range of signal intensity (Cercignani, 2011). Two major indices, peak height and location, are usually evaluated in histogram analysis. While the former reflects the change in a part of voxels which contribute to the maximum frequency, the latter is suggestive of rather a global change in voxels which contribute to the maximum frequency (Cercignani et al., 2001). This might suggest that there remained voxels with low FA values left undiscovered by the voxel-based analysis. Additional indices that can be evaluated include skewness (the magnitude of symmetry of the histograms) and kurtosis (peakness of histograms) (Mori et al., 2008). Histogram analysis of DTI has been successfully used in brain tumor classification (Wang et al., 2012), investigation of clinical correlates in leukoariosis (Della Nave et al., 2007) and multiple sclerosis (Cercignani et al., 2001), differentiation between ischemic and non-ischemic patients with moyamoya disease (Mori et al., 2008), evaluation of traumatic brain inury (Marquez de la Plata et al., 2011), and so on. In this study, histogram analysis enabled a discrimination between the patients and normal subjects by its peak position, which is suggestive of its applicability in the evaluation of integrity of brain parenchyma in MDD. When the cut-off value for the peak position of an FA histogram is 0.2, the sensitivity and specificity in distinguishing the patients from normal subjects are 0.89 and 0.74, respectively, as derived from ROC analysis (www.statsdirect.com). The strengths of histogram analysis include its ability to test many thousands of voxels as well as its robust statistical power (Della Nave et al., 2007). Its drawback is limited topographic information.

Because this study is an exploratory study, tests of correlation were performed without correction for multiple comparisons. A number of significant correlations between the FA values and the clinical variables were observed. The finding of positive correlation between the FA values and the clinical variables, especially clinical severity, is unusual. It is possible that the results of tests of correlation are inflated by Type I error associated with multiple comparisons (Gordi and Khamis., 2004). If corrected for multiple comparisons, no pairs with significant correlation would persist. Added to this, the slope of the regression lines might have been modified, and the correlation coefficient values might have been artificially increased, by the outliers (Hatch and Prihoda., 1992). On the other hand, if these correlations are considered as true correlations, the observation of difference in the pattern of correlation among the regions would suggest variation in the pattern of injury among the regions. Negative correlation between the duration of current disease episode and the FA value of the right frontal white matter ($x = 12$, $y = 43$, $z = -18$) would be indicative of impaired frontal white matter integrity with disease duration; and may reflect advancement of axon and/ or myelin injury with time. Positive correlation between disease duration and the regional FA values may be due to alteration in the local microenvironment by the long disease process or previous antidepressant medication. First, patients with long disease duration are exposed to chronic stress. Chronic stress has been demonstrated to contribute to frontostriatal regeneration and reductions in the length and branch numbers of apical dendrites, particularly in the anterior cingulate cortex (Radley et al., 2004). As dendrite formation and increased synaptic density are associated with decrease in the FA, the dendritic changes induced by chronic stress could in turn present with a relative

increase in the FA (Baloch et al., 2009; Taylor et al., 2011). However, owing to difference in histological composition between the two structures, the finding of anterior cingulate cortex may not plausibly explain the positive correlation between the FA value of the left anterior limb of the internal capsule and disease duration. Second, in this study, eight patients (those with long disease duration) had a previous history of antidepressant medication. Considering the half-lives of antidepressants, these patients were determined as being free of medication effects. However, the possibility that these patients' tissue microenvironment was modified and/ or aggressively treated by previous medication cannot be completely excluded. The significant positive correlation between the regional FA values and clinical severity might be due to astrocytic hypertrophy. Although the evidence is still limited, a recent autopsy report that investigated the white matter underlying anterior cingulate cortex of depressed suicidal patients has revealed an increase in the volume of astrocytic processes (representative of astrocytic hypertrophy) in the white matter (Torres-Platas et al., 2011). If it is assumed that astrocytic hypertrophy also occurs in the other white matter regions involved in MDD and that the degree of hypertrophy is severe enough to induce an increase in the regional FA values, the finding of FA increase with disease severity would be explained.

A few limitations of this study need to be addressed. First, correction for eddy current-induced distortion was not performed. This resulted in an imperfect match between the white matter masks constructed from the anatomical images (MPRAGE) and the FA and MD maps. Estimation of the average displacement between the MPRAGE images and the FA maps revealed an average shift of 0.91, 2.18, and 0.30 mm along the x, y, and z

directions, respectively. Nevertheless, the magnitude of displacement did not vary significantly between the patients and control subjects, so as to maintain validity of the analytical method for evaluation of global brain parenchymal or white matter abnormalities. Second, the slice thickness used for DTI was 5 mm, and the interslice gap was 1.5 mm. These parameters were chosen so as to allow acquisition of all necessary sequences in clinically acceptable scan time. Ideally, thinner slices without interslice gap are desired. Third, DSM-IV-TR was used to diagnose MDD in the patients, whereas MINI was used to exclude psychiatric diseases in normal subjects. Hence, there might be a question about potential bias arising from the use of different diagnostic assessment methods between the two groups. However, the possibility is considered unlikely as MINI is well-designed to be used to rule out psychiatric diseases, and is compatible with DSM-IV-TR (Sheehan et al., 1998).

In conclusion, this study evaluated the integrity of the brain parenchyma in non-geriatric patients with MDD by using two different analytical methods of DTI. The findings suggest an impaired integrity of the frontal-subcortical circuits and cerebro-cerebellar connections, which are known or thought to mediate human behavior. Consistency in the distribution of abnormalities is lacking among the studies including the current report, which may suggest spatial heterogeneity of the abnormalities in MDD. The peak position of the FA histograms may be used as supplementary to voxel-based analysis, in evaluation of the brain parenchymal integrity in MDD.

Acknowledgement

The authors are greatly indebted to the anonymous reviewers for the invaluable comments. This study was supported by (1) Creation of Innovation Centers for Advanced Interdisciplinary Research Areas Program of Project for Developing Innovation Systems of the Ministry of Education, Culture, Sports, Science and Technology, the Japanese Government, and (2) the Grant-in-aid for Scientific Research by the Japan Society for Promotion of Science (Project number 20591430).

References

Alexopoulos, G.S., Kiosses, D.N., Choi, S.J., Murphy, C.F., Lim, K.O., 2002. Frontal white matter microstructure and treatment response of late-life depression: A preliminary study. American Journal of Psychiatry 159, 1929–1932.

Alexopoulos, G.S., Murphy, C.F., Gunning-Dixon, F.M., Latoussakis, V., Kanellopoulos, D., Klimstra, S., Lim, K.O., Hoptman, M.J., 2008. Microstructural white matter abnormalities and remission of geriatric depression. American Journal of Psychiatry 165, 238–244.

Bae, J.N., MacFall, J.R., Krishnan, K.R., Payne, M.E., Steffens, D.C., Taylor, W.D., 2006. Dorsolateral prefrontal cortex and anterior cingulate cortex white matter alterations in late-life depression. Biological Psychiatry 60, 1356–1363.

Baloch, S., Verma, R., Huang, H., Khurd, P., Clark, S., Yarowsky, P., Abel, T., Mori, S., Davatzikos, C., 2009. Quantification of brain maturation and growth patterns in C57BL/6J mice via computational neuroanatomy of diffusion tensor images. Cerebral Cortex 19, 675–687.

Basser, P.J., Pierpaoli, C., 1996. Microstructural and physiological features of tissues elucidated by quantitative-diffusion tensor MRI. Journal of Magnetic Resonance B 111, 209 – 219.

Beaulieu, C., 2011. What makes diffusion anisotropic in the newvous system? In: Jones, D.K. (Ed.), Diffusion MRI: theory, methods, and applications. Oxford University Press, New York, pp. 92-109.

Beauregard, M., Leroux, J. M., Bergman, S., Arzoumanian, Y., Beaudoin, G., Bourgouin, P., Stip, E.,1998. The functional neuroanatomy of major depression: an FMRI study using an emotional activation paradigm. Neuroreport 14, 3253-3258.

Blood, AJ., Iosifescu, D.V., Makris, N., Perlis, R.H., Kennedy, D.N., Dougherty, D.D., Kim, B.W., Lee, M.J., Wu, S., Lee, S., Calhoun, J., Hodge, S.M., Fava, M., Rosen, B.R., Smoller, J.W., Gasic, G.P., Breiter, H.C., 2010. Microstructural abnormalities in subcortical reward circuitry of subjects with major depressive disorder. PLOS one 11, e13945.

Cercignani, M., Inglese, M., Pagani, E., Comi, G., Filippi, M., 2001. Mean diffusivity and fractional anisotropy histograms of patients with multiple sclerosis. American Journal of Neuroradiology 22, 952-958.

Cercignani, M., 2011. Strategies for patient-control comparison of diffusion MR data. In: Jones, D.K. (Ed.), Diffusion MRI: theory, methods, and applications. Oxford University Press, New York, pp. 485-499.

Della Nave, R., Foresti, S., Pratesi, A., Ginestroni, A., Inzitari, M., Salvadori, E., Giannelli, M., Diciotti, S., Inzitari, D., Mascalchi, M., 2007. Whole-brain histogram and voxel-based analyses of diffusion tensor imaging in patients with leukoariosis: correlation with motor and cognitive impairment. American Journal of Neuroradiology 28, 1313-1319.

Diamond, A., 2000. Close interrelation of motor development and cognitive development and of the cerebellum and prefrontal cortex. Child Development 71, 44-56.

Dolan, R.J., Bench, C.J., Brown, R.G., Scott, L.C., Friston, K.J., Frackowiak, R.S., 1992. Regional cerebral blood flow abnormalities in depressed patients with cognitive impairment. Journal of Neurology, Neurosurgery & Psychiatry 55, 768-773.

Egger, K., Schocke, M., Weiss, E., Auffinger, S., Esterhammer, R., Goebel, G., Walch, T., Mechtcheriakov, S., Marksteiner, J., 2008. Pattern of brain atrophy in elderly patients with depression revealed by voxel-based morphometry. Psychiatry Research 164, 237–244.

Fatemi, S.H., Laurence, J.A., Aragi-Niknam, M., Stary, J.M., Schulz, S.C., Lee, S., Gottesman, I.I., 2004. Glial fibrillary acidic protein is reduced in cerebellum of subjects with major depression, but not schizophrenia. Schizophrenia Research 69, 317-323.

Fujimoto, T., Takeuchi, K., Matsumoto, T., Fujita, S., Honda, K., Higashi, Y., Kato, N., 2008. Metabolic changes in the brain of patients with late-onset major depression. Psychiatry Research 164, 48-57.

Gordi, T., Khamis, H., 2004. Simple Solution to a Common Statistical Problem: Interpreting Multiple Tests. Clinical Therapeutics 26, 780-786.

Graff-Guerrero, A., González-Olvera, J., Mendoza-Espinosa, Y., Vaugier, V., García-Reyna, J.C., 2004. Correlation between cerebral blood flow and items of the Hamilton Rating Scale for Depression in antidepressant-naive patients. Journal of Affective Disorders 80, 55-63.

Greenberg, P.E., Stiglin, L.E., Finkelstein, S.N., Berndt, E.R., 1993.The economic burden of depression in 1990. Journal of Clinical Psychiatry 54, 405–418.

Guy, W., 1976. ECDEU Assessment Manual for Psychopharmacology. Rockville, MD: U.S. Department of Health, Education, and Welfare.

Hall, R.C.W., 1995. Global assessment of functioning: a modified scale. Psychosomatics 36, 267-275.

Hatch, J.P., Prihoda, T.J., 1992. The Effect of Influential Outliers on Parameter

Estimation in Regression Analysis. Biofeedback and Self-Regulation 17, 153-156.

Jones, D.K., Symms, M.R., Cercignani, M.C., Howard, R.J., 2005. The effect of filter size on the outcome of VBM analyses of DT-MRI data. Neuroimage 26, 546–554.

Kessler, R.C., Berglund, P., Demler, O., Jin, R., Koretz, D., Merikangas, K.R., Rush, A.J., Walters, E.E., Wang P.S., 2003. National Comorbidity Survey Replication. The epidemiology of major depressive disorder: Results from the National Comorbidity Survey Replication (NCS-R). The Journal of American Medical Association 289, 3095–3105.

Konarski, J.Z., McIntyre, R.S., Grupp, L.A., Kennedy, S. H., 2005. Is the cerebellum relevant in the circuitry of neuropsychiatric disorders? Journal of Psychiatry and Neuroscience 30, 178-186.

Korgaonkar, M.S., Grieve, S.M., Koslow, S.H., Gabrieli, J.D., Gordon, E., Williams, L.M., 2011. Loss of white matter integrity in major depressive disorder: Evidence using tract-based spatial statistical analysis of diffusion tensor imaging. Human Brain Mapping 32, 2161-2171.

Li, L., Ma, N., Li, Z., Tan, L., Liu, J., Gong, G., Shu, N., He, Z., Jiang, T., Xu, L., 2007. Prefrontal white matter abnormalities in young adult with major depressive disorder: A diffusion tensor imaging study. Brain Research 1168, 124–128.

Ma, N., Li, L., Shu, N., Liu, J., Gong, G., He, Z., Li, Z., Tan, L., Stone, W.S., Zhang, Z., Xu, L., Jiang, T., 2007. White matter abnormalities in first-episode, treatment-naive young adults with major depressive disorder. American Journal of Psychiatry 164, 823–826.

Malykhin, N., Concha, L., Seres, P., Beaulieu, C., Coupland, N.J., 2008. Diffusion tensor imaging tractography and reliability analysis for limbic and paralimbic white matter tracts. Psychiatry Research 164, 132–142.

Marquez de la Plata, C.D., Yang, F.G., Wang, J.Y., Krishnan, K., Bakhadirov, K., Paliotta, C., Aslan, S., Devous, M.D., Moore, C., Harper, C., McColl, R., Munro Cullum, C., Diaz-Arrastia, R., 2011. Diffusion tensor imaging biomarkers for traumatic axonal injury: analysis of three analytic methods. Journal of the International Neuropsychological Society 17, 24-35.

Montgomery, S.A., Åsberg, M., 1979. A new depression scale designed to be sensitive to change. British Journal of Psychiatry 134, 382–389.

Mori. N., Miki. Y., Fushimi, Y., Kikuta, K., Urayama, S., Okada, T., Fukuyama, H., Hashimoto, N., Togashi, K., 2008. Cerebral infarction associated with moyamoya disease: histogram-based quantitative analysis of diffusion tensor imaging — a preliminary study. Magnetic Resonance Imaging 26, 835-840.

Moseley, M., 2002. Diffusion tensor imaging and aging: a review. NMR in Biomedicine 15, 553 – 560.

Nagesh. V., Tsien, C.I., Chenevert, T.L., Ross, B.D., Lawrence, T.S., Junick, L., Cao, Y., 2008. Radiation-induced changes in normal-appearing white matter in patients with cerebral tumors: a diffusion tensor imaging study. International Journal of Radiation Oncology Biology Physics 70, 1002 – 1010.

Nobuhara, K., Okugawa, G., Sugimoto, T., Minami, T., Tamagaki, C., Takase, K., Saito, Y., Sawada, S., Kinoshita, T., 2006. Frontal white matter anisotropy and symptom severity of

late-life depression: A magnetic resonance diffusion tensor imaging study. Journal of Neurology, Neurosurgery and Psychiatry 77, 120–122.

Ouyang, X., Tao, H.J., Liu, H.H., Deng, Q.J., Sun, Z.H., Xu, L., Liu, Z.N., Xue, Z.M., 2011. White matter integrity deficit in treatment-naïve adult patients with major depressive disorder. East Asian Archives of Psychiatry 21, 5-9.

Radley, J. J., Sisti, H. M., Hao, J., Rocher, A.B., McCall, T., Hof, P.R., McEwen, B.S., Morrison, J.H., 2004. Chronic behavioral stress induces apical dendritic reorganization in pyramidal neurons of the medial prefrontal cortex. Neuroscience 125, 1–6.

Regenold, W.T., Phatak, P., Marano, C.M., Gearhart, L., Viens, C.H., Hisley, K.C., 2007. Myelin staining of deep white matter in the dorsolateral prefrontal cortex in schizophrenia, bipolar disorder, and unipolar major depression. Psychiatry Research 151, 179–188.

Sala, S., Agosta, F., Pagani, E., Copetti, M., Comi, G., Filippi, M., 2012. Microstructural changes and atrophy in brain white matter tracts with aging. Neurobiology of Aging 33, 488-498.

Sheehan, D.V., Lecrubier, Y., Sheehan, K.H., Amorim, P., Janavs, J., Weiller, E., Hergueta, T., Baker, R., Dunbar, G.C., 1998. The Mini-International Neuropsychiatric Interview (M.I.N.I): the development and validation of a structured diagnostic psychiatric interview for DSM-IV and ICD-10. The Journal of Clinical Psychiatry 59, 22-33.

Shimony, J.S., Sheline, Y.I., D'Angelo, G., Epstein, A.A., Benzinger, T.L., Mintun, M.A., McKinstry, R.C., Snyder, A.Z., 2009. Diffuse microstructural abnormalities of normal-appearing white matter in late life depression: A diffusion tensor imaging study. Biological Psychiatry 66, 245–252.

Sijens, P.E., Mostert, J.P., Irwan, R., Potze, J.H., Oudkerk, M., Keyser J.D., 2008. Impact of fluoxetine on the human brain in multiple sclerosis as quantified by proton magnetic resonance spectroscopy and diffusion tensor imaging. Psychiatry research: Neuroimaging 164, 274-282.

Strick, P.L., Dum, R.P., Fiez, J.A., 2009. Cerebellum and nonmotor function. The Annual Review of Neuroscience 32, 413-434.

Taoka, T., Kin, T., Nakagawa, H., Hirano, M., Sakamoto, M, Wada, T., Takayama, K., Wuttikul, C., Iwasaki, S., Ueno, S., Kichikawa, K., 2007. Diffusivity and diffusion anisotropy of cerebellar peduncles in cases of spinocerebellar degenerative disease. Neuroimage 37, 387-393.

Taylor, W.D., MacFall, J.R., Boyd, B., Payne, M.E., Sheline, Y.I., Krishnan, K.R.R., Doraiswamy, P.M., 2011. One-year change in anterior cingulate cortex white matter microstructure: relationship with late-life depression outcomes. American Journal of Geriatric Psychiatry 19, 43-52.

Taylor, W.D., MacFall, J.R., Payne, M.E., McQuoid, D.R., Provenzale, J.M., Steffens, D.C., Krishnan, K.R., 2004. Late-life depression and microstructural abnormalities in dorsolateral prefrontal cortex white matter. American Journal of Psychiatry 161, 1293–1296.

Tekin, S., Cummings, J.L., 2002. Frontal-subcortical neuronal circuits and clinical neuropsychiatry: an update. Journal of Psychosomatic Research 53, 647–654.

Tha, K.K., Terae, S., Yabe, I., Miyamoto, T., Soma, H., Zaitsu, Y., Fujima, N., Kudo, K., Sasaki, H., Shirato, H., 2010. Microstructural white matter abnormalities of multiple

system atrophy: in vivo topographic illustration by using diffusion-tensor MR imaging. Radiology 255, 563-569.

Torres-Platas, S. G., Hercher, C., Davoli, M. A., Maussion, G., Labonte´, B., Turecki, G., Mechawar, N., 2011. Astrocytic Hypertrophy in Anterior Cingulate White Matter of Depressed Suicides. Neuropsychopharmacology 36, 2650–2658.

Tsopelas, C., Stewart, R., Sawa, G.M., Brayne, C., Ince, P., Thomas, A., Matthews, F.E., Medical Research Council Cognitive Function and Ageing Study, 2011. Neuropathological correlates of late-life depression in older people. The British Journal of Psychiatry 198, 109-114.

Uranova, N.A., Vostrikov, V.M., Orlovskaya, D.D., Rachmanova, V.I., 2004. Oligodendroglial density in the prefrontal cortex in schizophrenia and mood disorders: a study from the Stanley neuropathology consortium, Schizophrenia Research 67, 269–275.

Videbech, P., Ravnkilde, B., Pedersen, A.R., Egander, A., Landbo. B., Rasmussen NA, Andersen, F., Stødkilde-Jørgensen, H., Gjedde, A., Rosenberg, R., 2001. The Danish PET/depression project: PET findings in patients with major depression. Psychological Medicine 31, 1147-1158.

Wang, S., Kim, S., Zhang, Y., Wang, L., Lee, E. B., Syre, P., Poptani, H., Melhem, E. R., Lee, J. Y., 2012. Determination of grade and subtypes of meningiomas by using histogram analysis of diffusion-tensor imaging metrics. Radiology 262, 584-592.

Waxman, H.M., Carner, E.A., Dubin, W., Klein, M., 1982. Geriatric psychiatry in the emergency department: characteristics of geriatric and non-geriatric admissions. Journal of the American Geriatrics Society 30, 427-432.

Williams, J.B., 1988. A structured interview guide for the Hamilton Depression Rating Scale. Archives of General Psychiatry 45, 742–747.

Wu, F., Tang, Y., Xu, K., Kong, L., Sun, W., Wang, F., Kong, D., Li, Y., Liu, Y., 2011. White matter abnormalities in medication-naive subjects with a single short-duration episode of major depressive disorder. Psychiatry Research 191, 80-83.

Yang, Q., Huang, X., Hong, N., Yu, X., 2007. White matter microstructural abnormalities in late-life depression. International Psychogeriatrics 19, 757–766.

Yoo, S.Y., Jang, J.H., Shin, Y-H., Kim, D.J., Park, H-J., Moon, W-J., Chung, E.C., Lee, J-M., Kim, I.Y., Kim, S.I., Kwon, J.S., 2007. White matter abnormalities in drug-naïve patients with obsessive-compulsive disorder: a diffusion tensor study before and after citalopram treatment. Acta Psychiatrica Scandinavica 116, 211-219.

Zhu, X., Wang, X., Xiao, J., Zhong, M., Liao, J., Yao, S., 2011. Altered white matter integrity in first-episode, treatment-naïve young adults with major depressive disorder: a tract-based spatial statistics study. Brain research 1369, 223-229.

Zou. K., Huang, X., Li, T., Gong, Q., Li, Z., Ou-Yang, L., Deng, W., Chen, Q., Li, C., Ding, Y., Sun, X., 2008. Alterations of white matter integrity in adults with major depressive disorder: A magnetic resonance imaging study. Journal of Psychiatry &Neuroscience 33, 525–530.

Figures

Fig. 1. The results of voxel-by-voxel comparison of FA values between the patients and control subjects, superimposed on a T1-weighted template. Clusters with significant decrease in FA values (uncorrected *P <0.001*, minimum cluster size = 50 voxels) are observed in the patients, in the right frontal white matter {(i) MNI coordinates: x = 12, y = 43, z = -18, cluster size = 70 voxels, *t = 4.34*; (ii) MNI coordinates: x = 37, y = -19, z = 59, cluster size = 100 voxels, *t = 4.43*}, left frontal white matter (MNI coordinates: x = -24, y = -21, z = 34, cluster size = 135 voxels, *t = 4.53*), right anterior limb of internal capsule (MNI coordinates: x = 17, y = 18, z = -9, cluster size = 111 voxels, *t = 4.63*), left anterior limb of internal capsule (MNI coordinates: x = -14, y = 14, z = 9, cluster size = 135 voxels, *t = 4.62*), left putamen (MNI coordinates: x = -24, y = -7, z = 7, cluster size = 74 voxels, *t = 4.12*), the mediodorsal nucleus of right thalamus (MNI coordinates: x = 7, y = -14, z = 8, cluster size = 138 voxels, *t = 4.98*), right cerebellar hemisphere (MNI coordinates: x = 22, y = -48, z = -27, cluster size = 83 voxels, *t = 4.14*), and left cerebellar hemisphere (MNI coordinates: x = -3, y = -49, z =-25, cluster size = 50 voxels, *t = 4.17*). Look-up table represents the *t* values. L and R represent the left and right sides, respectively.

Fig. 2. The mean FA histograms of the patients (solid line) and control subjects (dotted line). The average number of normalized voxels is plotted against the logarithm of the FA values. The peak position of FA histogram of the patients is significantly lower than that of normal subjects (*P=0.00097*). The peak height of FA histograms does not vary significantly.

Fig. 3. The mean MD histograms of the patients (solid line) and control subjects (dotted line). The average number of normalized voxels is plotted against the logarithm of the MD values. No significant difference in the peak position or height of MD histograms is observed.

Fig. 4. Scatterplots showing correlation between the abnormal DTI indices and the clinical variables. Correlations between (A) the FA values of right frontal white matter (x = 12, y = 43, z = -18) and the duration of current disease episode, (B) the FA values of the left anterior limb of internal capsule and total disease duration, (C) the peak positions of FA histograms and total disease duration, (D) the peak positions of FA histograms and the duration of current disease episode, (E) the FA values of the right frontal white matter (x = 37, y = -19, z = 59) and the GAF, (F) the FA values of the right anterior limb of internal capsule and the GAF, and (G) the FA values of the right cerebellar hemisphere and the HDRS-17, are shown. White circles represent the medication-naïve patients. Black circles represent the patients who had a previous history of antidepressant medication. The solid lines represent the mean, and the dashed lines represent 95% confidence interval for the mean predicted value. Abbreviations: a.u. = arbitrary unit; FA = fractional anisotropy; GAF = global assessment of functioning; HDRS-17 = 17-item Hamilton depression rating scale.

Tables

Table 1. The demographic characteristics of the patients and normal subjects

	Patients (*n=19*)	Control subjects (*n=19*)	*P*-value
Age	38.6 ± 13.5 years (20-61)*	36.5 ± 12.5 years (22-60)*	*0.613*[#]
Gender (men/women)	12/7	13/6	*0.729*[♣]
Previous history of antidepressant medication (Present/absent)	8/11	-	-
Previous episodes (Present/absent)	5/14	-	-
Total disease duration	18.37 ± 28.17 months (1-96)*	-	-
Duration of current episode	5.89 ± 5.69 months (1-24)*	-	-
HDRS-17	19.00 ± 4.00 (11-26)*	-	-
GAF	43.79 ± 9.90 (28-58)*	-	-
MADRS	26.21 ± 5.57 (20-39)*	-	-
CGI-S	4.68 ± 0.89 (3-6)	-	-

*Data are presented in mean ± standard deviation (range).

The statistical significance was evaluated by using two-sample *t* test[#] or χ^2 test[♣].

Abbreviations: HDRS-17 =17-item Hamilton depression rating scale; GAF = global assessment of functioning; MADRS = Montgomery-Ásberg depression rating scale; CGI-S = clinical global impression-severity.

Table 2. Tests of correlation between the abnormal DTI indices and the clinical variables.

	Correlation coefficients (*P* value)						
	Total disease duration	Duration of current episode	HDRS-17	GAF	MADRS	CGIS	Age
Clusters with significant decrease in FA							
Right frontal white matter	- 0.296	- 0.482	0.084	-0.012	-0.117	-0.006	0.188
(x = 12, y = 43, z = -18)	*(0.219)*	*(0.036)**	*(0.732)*	*(0.960)*	*(0.634)*	*(0.980)*	*(0.440)*
Right frontal white matter	0.080	0.318	0.135	-0.462	0.413	0.412	-0.392
(x = 37, y = -19, z = 59)	*(0.746)*	*(0.184)*	*(0.583)*	*(0.046)**	*(0.079)*	*(0.080)*	*(0.097)*
Left frontal white matter	0.247	0.087	0.160	-0.367	0.351	0.377	0.109
	(0.308)	*(0.723)*	*(0.512)*	*(0.122)*	*(0.141)*	*(0.112)*	*(0.657)*

Right anterior limb of internal capsule	0.335	0.163	- 0.117	-0.479	0.229	0.363	-0.070
	(0.160)	*(0.506)*	*(0.634)*	*(0.038)**	*(0.345)*	*(0.127)*	*(0.775)*
Left anterior limb of internal capsule	0.483	- 0.011	0.078	-0.410	0.384	0.359	- 0.308
	*(0.036)**	*(0.964)*	*(0.750)*	*(0.081)*	*(0.105)*	*(0.131)*	*(0.200)*
Left putamen	- 0.112	- 0.191	- 0.026	-0.276	0.120	0.327	- 0.397
	(0.648)	*(0.433)*	*(0.915)*	*(0.252)*	*(0.626)*	*(0.171)*	*(0.092)*
Mediodorsal nucleus of the right thalamus	0.434	- 0.116	0.052	-0.248	0.152	0.326	- 0.424
	(0.063)	*(0.635)*	*(0.831)*	*(0.307)*	*(0.535)*	*(0.173)*	*(0.071)*
Right cerebellar hemisphere	- 0.073	- 0.034	0.525	-0.383	0.272	0.345	0.258
	(0.767)	*(0.891)*	*(0.021)**	*(0.106)*	*(0.260)*	*(0.148)*	*(0.286)*
Left cerebellar hemisphere	0.168	0.214	0.434	-0.274	0.252	0.177	0.498
	(0.492)	*(0.380)*	*(0.063)*	*(0.257)*	*(0.297)*	*(0.470)*	*(0.030)**
Peak position of FA histogram	0.576	0.550	- 0.020	-0.087	0.402	0.040	0.219

	*(0.010)**	*(0.015)**	*(0.936)*	*(0.723)*	*(0.088)*	*(0.869)*	*(0.368)*

*indicates statistical significance (*P <0.05*).

Abbreviations: HDRS-17 =17-item Hamilton depression rating scale; GAF = global assessment of functioning; MADRS = Montgomery-Åsberg depression rating scale; CGI-S = clinical global impression-severity.

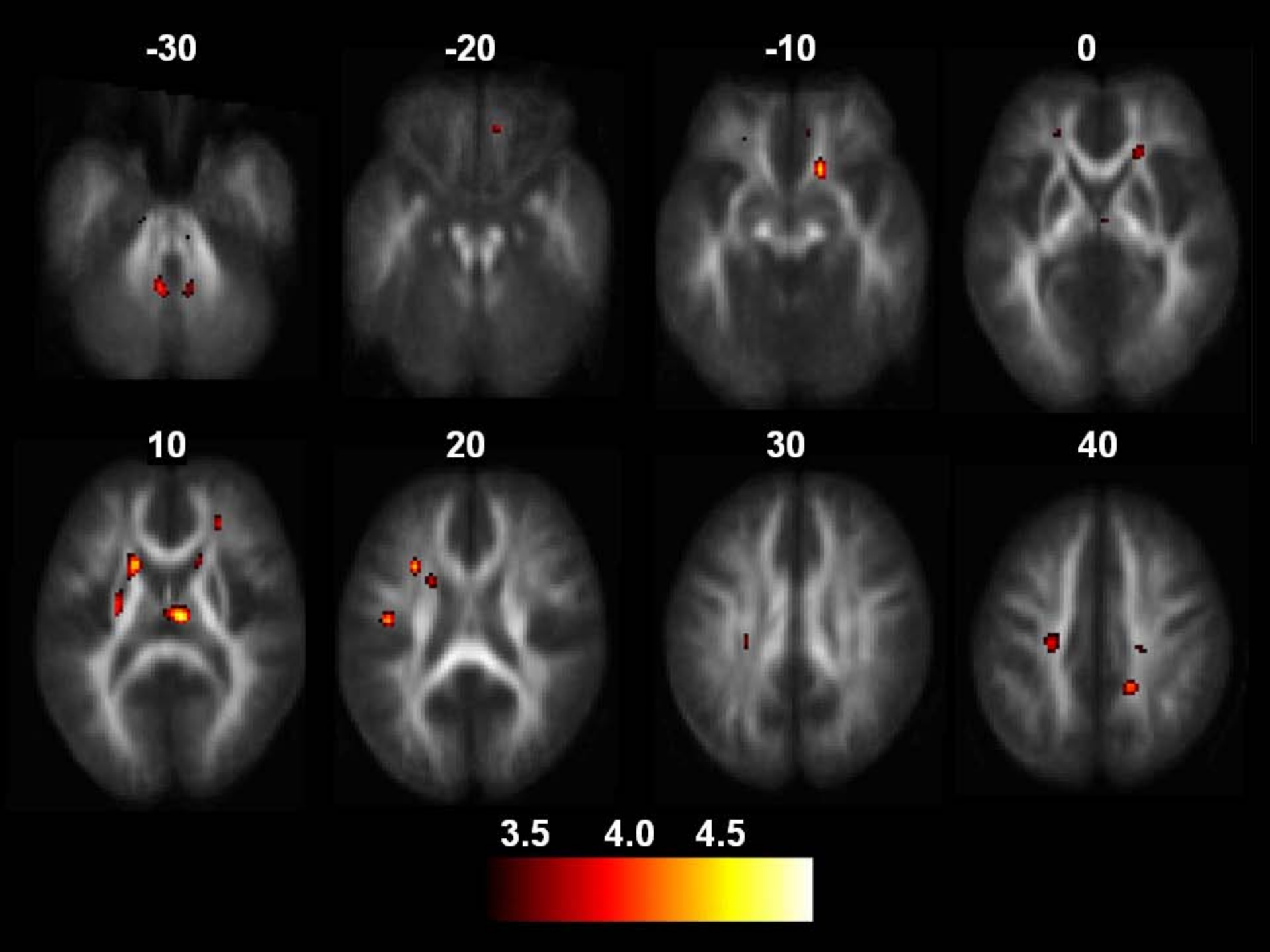
-30
-20
-10
0
10
20
30
40
3.5
4.0
4.5

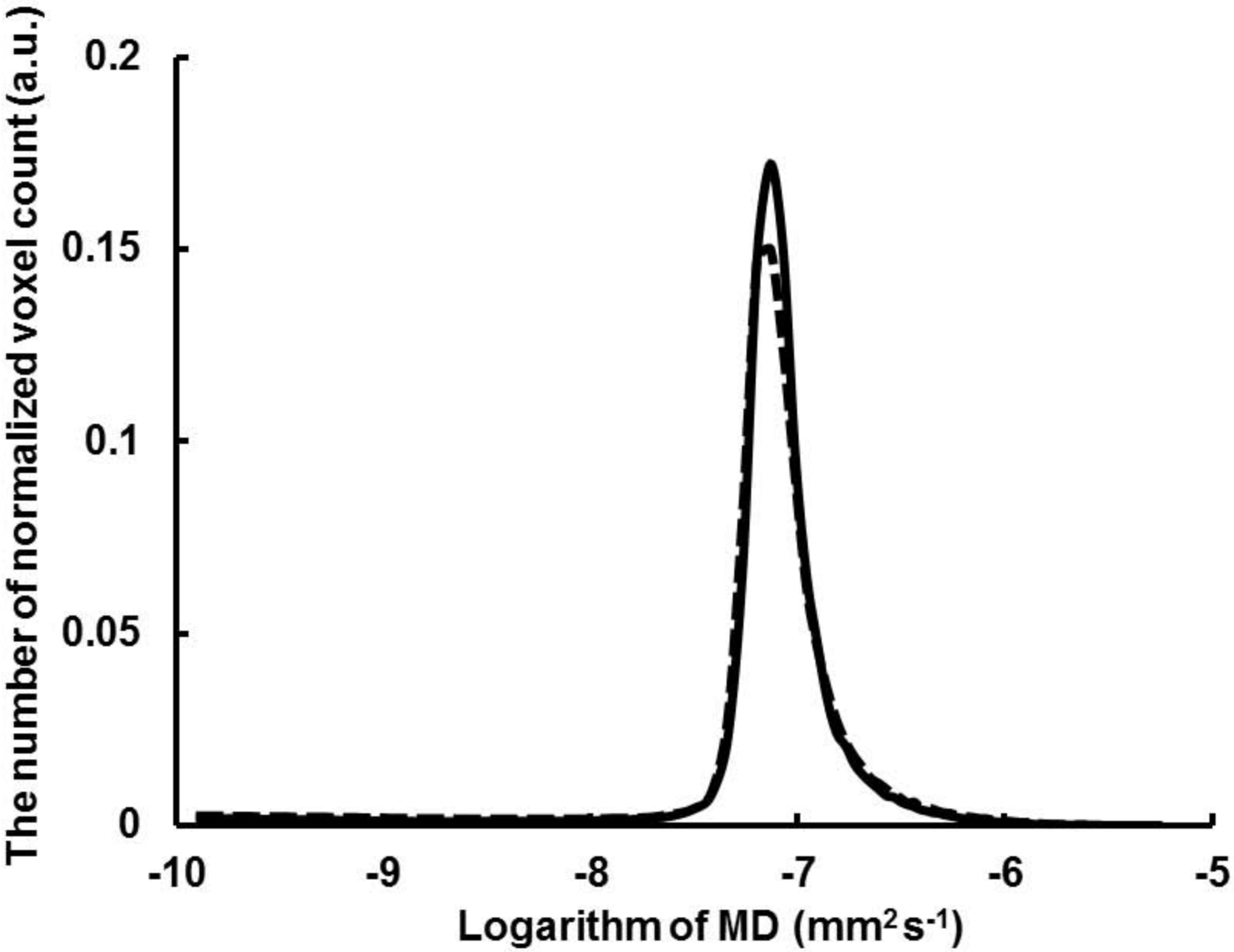
The number of normalized voxel count (a.u.)
0.2
0.15
0.1
0.05
0
-10
-9
-8
-7
-6
-5
Logarithm of MD (mm2 s-1)

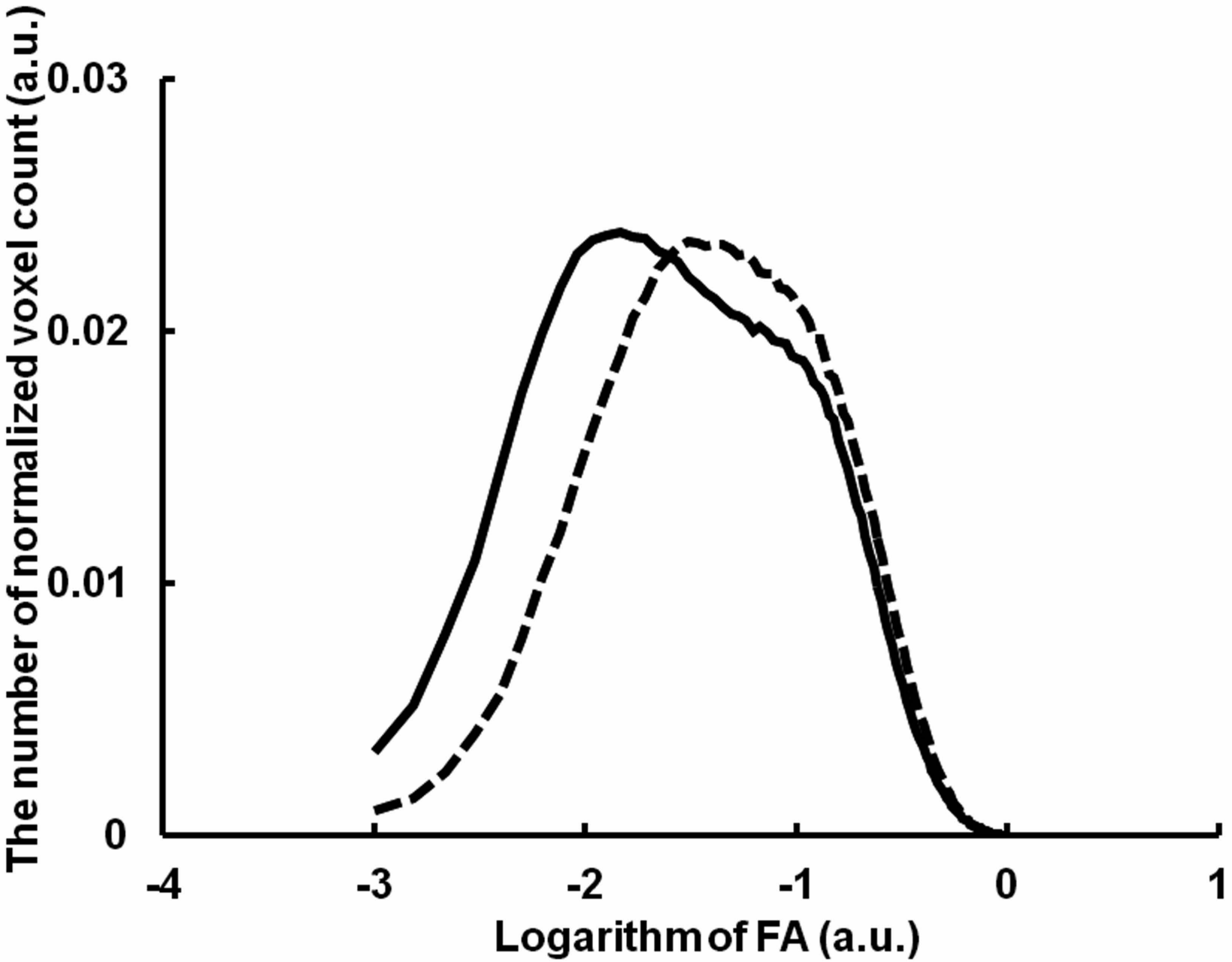
The number of normalized voxel count (a.u.)
0.03
0.02
0.01
0
-4
-3
-2
-1
0
1
Logarithm of FA (a.u.)

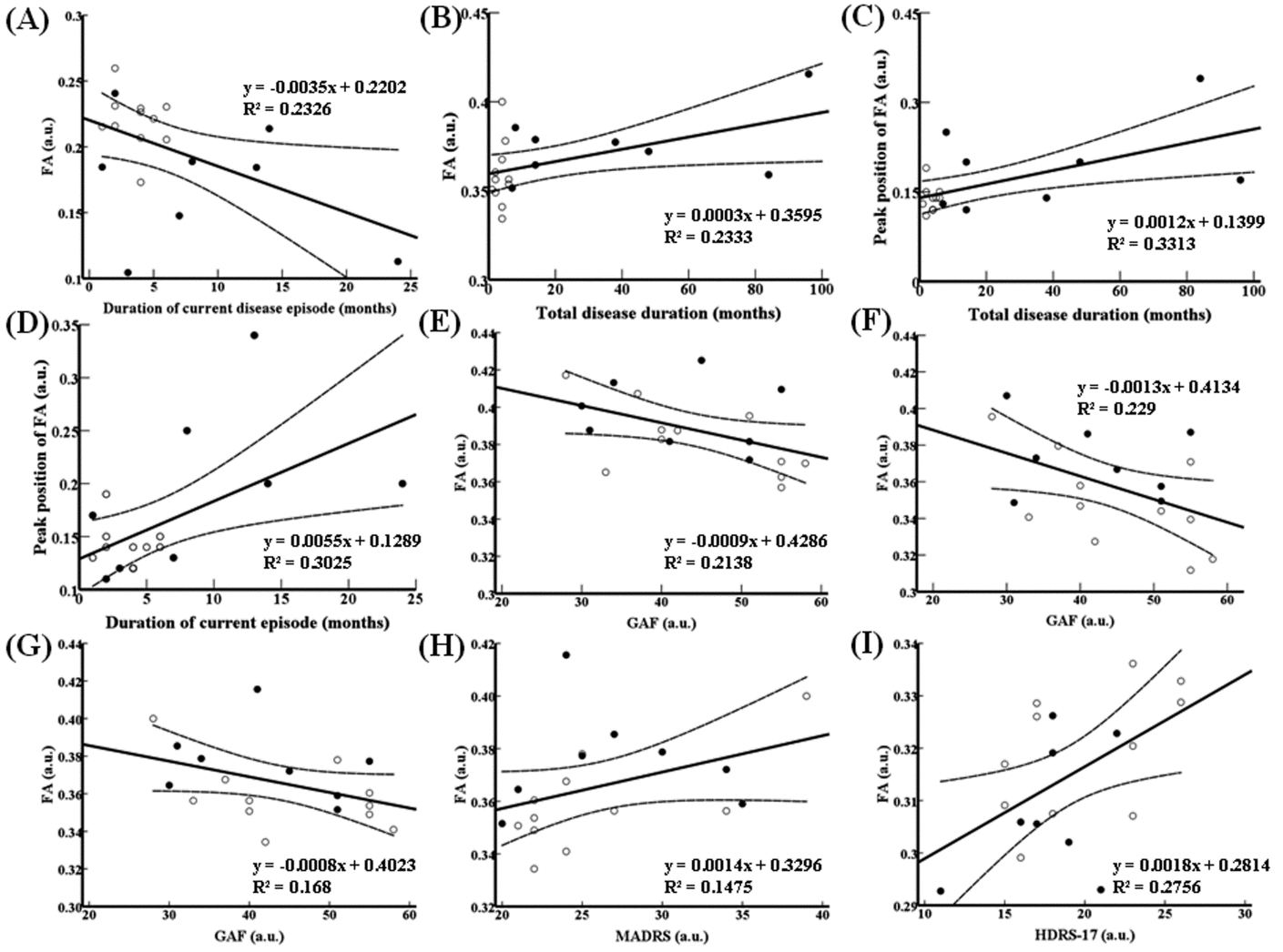
(A)
y = -0.0035x + 0.2202
R² = 0.2326
FA (a.u.)
Duration of current disease episode (months)
(B)
y = 0.0003x + 0.3595
R² = 0.2333
FA (a.u.)
Total disease duration (months)
(C)
y = 0.0012x + 0.1399
R² = 0.3313
Peak position of FA (a.u.)
Total disease duration (months)
(D)
y = 0.0055x + 0.1289
R² = 0.3025
Peak position of FA (a.u.)
Duration of current episode (months)
(E)
y = -0.0009x + 0.4286
R² = 0.2138
FA (a.u.)
GAF (a.u.)
(F)
y = -0.0013x + 0.4134
R² = 0.229
FA (a.u.)
GAF (a.u.)
(G)
y = -0.0008x + 0.4023
R² = 0.168
FA (a.u.)
GAF (a.u.)
(H)
y = 0.0014x + 0.3296
R² = 0.1475
FA (a.u.)
MADRS (a.u.)
(I)
y = 0.0018x + 0.2814
R² = 0.2756
FA (a.u.)
HDRS-17 (a.u.)